Volume 14 | Issue 1 Spring 2018

Acoustics Today

A Publication of the Acoustical Society of America

The Inaudible Rumble of Volcanic Eruptions

Also In This Issue

The Inaudible Rumble of Volcanic Eruptions

Robin S. Matoza

Postal:
Department of Earth Science and
Earth Research Institute
University of California, Santa Barbara
Santa Barbara, California 93106-9630
USA

Email:
rmatoza@ucsb.edu

David Fee

Postal:
Wilson Alaska Technical Center
Alaska Volcano Observatory
Geophysical Institute
University of Alaska, Fairbanks
Fairbanks, Alaska 99775-7320
USA

Email:
dfee1@alaska.edu

Volcanic eruptions produce powerful infrasound that can be used to monitor and mitigate volcanic hazards.

Introduction and Context

There are approximately 1,500 volcanoes worldwide that are considered *potentially active*, defined as a volcano at which an eruption has occurred within the past 10,000 years (Global Volcanism Program, 2013; **Figure 1**). Eruptions are common; for example, more than 50 eruptions have occurred in the United States in the past 31 years (National Academies of Sciences, Engineering, and Medicine, 2017). Approximately 500 million people worldwide are directly exposed to volcanic hazards. This number is steadily increasing as population density grows in areas near volcanoes. Fortunately, many eruptions are preceded by unrest, and volcano-monitoring scientists use an array of different ground-based, airborne, and spaceborne techniques to detect this unrest, track eruption progression, build understanding of how volcanoes work, and provide timely warnings where possible. However, many potentially active volcanoes are located in remote and inhospitable regions of the planet where it is challenging to install and maintain dedicated local monitoring instruments. Although such volcanoes may be located in sparsely populated areas, explosive eruptions at these remote volcanoes can inject large volumes of ash into heavily traveled aviation routes, posing a major societal and economic hazard (Casadevall, 1994). Volcanic ash consists of tiny particles (<2-mm grain size) of solid rock, with a melting temperature below the operating temperature of jet engines. Encounters between volcanic ash and aircraft have resulted in engine

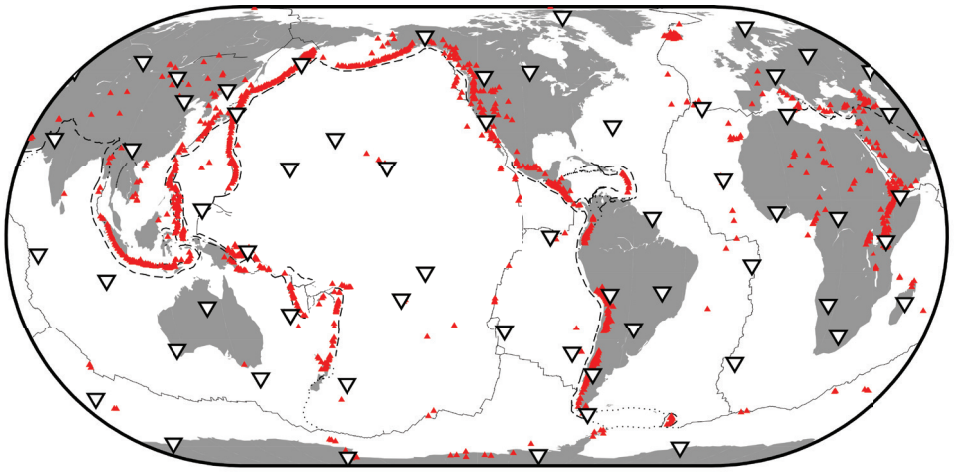

Figure 1. *Global potentially active volcanoes (eruption in past 10,000 years;* ***red triangles****), tectonic plate boundaries (****black lines****:* ***solid****, ridge plate boundary type;* ***dashed****, trench plate boundary type;* ***dotted,*** *transform plate boundary type), and the planned 59-station International Monitoring System (IMS) infrasound network (****open inverted triangles****). At present, 49 stations are operational. Each infrasound station consists of a small array of infrasonic sensors deployed in a variety of spatial configurations with maximum dimensions of 1-2 km across the ground surface. The average station spacing for the complete network will be about 2,000 km. Modified from Matoza et al. (2017), with permission.*

failure and damage to commercial airlines; consequently, volcanic ash clouds lead to extensive flight cancellations, delays, and economic losses (e.g., the 2010 eruption of Eyjafjallajökull, Iceland).

For example, Alaska is home to 130 potentially active volcanoes, of which more than 50 have erupted in historical times (**Figure 2**). Volcanoes in this region are capable of sudden, explosive, ash-cloud forming eruptions, which are potentially hazardous to aircraft along this heavily traveled air corridor. Monitoring of these volcanoes is performed at the Alaska Volcano Observatory (AVO) by integrating multiple ground-based and satellite-monitoring technologies. However, Aleutian Island volcanoes along the western part of Alaska (**Figure 2a**) in particular represent a formidable monitoring challenge because of their remote locations and harsh weather. Thus, many Aleutian volcanoes are not instrumented.

Infrasound is atmospheric sound with frequencies between ~0.01 and 20 Hz, that is, below the lower frequency limit of human hearing. The infrasonic frequency band contains the majority of acoustic energy emitted by volcanoes. Over the past two decades, infrasound technology has emerged as a new ground-based method to detect and quantify volcanic eruptions at both local and remote distances from volcanoes.

The recent progress in volcano-infrasound research has been driven in part by the opening for signature of the Comprehensive Nuclear-Test-Ban Treaty (CTBT) in 1996. The treaty calls for a verification regime to be established, of which the International Monitoring System (IMS) is one element. The IMS infrasound network (**Figure 1**, ***open inverted triangles***) is designed to detect atmospheric nuclear explosions anywhere on the planet (Christie and Campus, 2010). Construction of the IMS has led to rapid advances in infrasound technology (e.g., improvements in instrumentation, signal-processing methods, and infrasound propagation modeling), which have been transferred and adapted to volcanology.

The IMS infrasound network regularly records signals from large explosive volcanic eruptions worldwide. In addition, numerous other infrasound stations have been deployed near volcanoes or in volcanic regions to study and monitor volcanoes. Sensor acquisition geometries have included networks of individual infrasound sensors, infrasound arrays, networks of infrasound arrays like the IMS, and colocated seismic and acoustic (seismo-acoustic) stations. For example, the EarthScope USArray Transportable Array has now

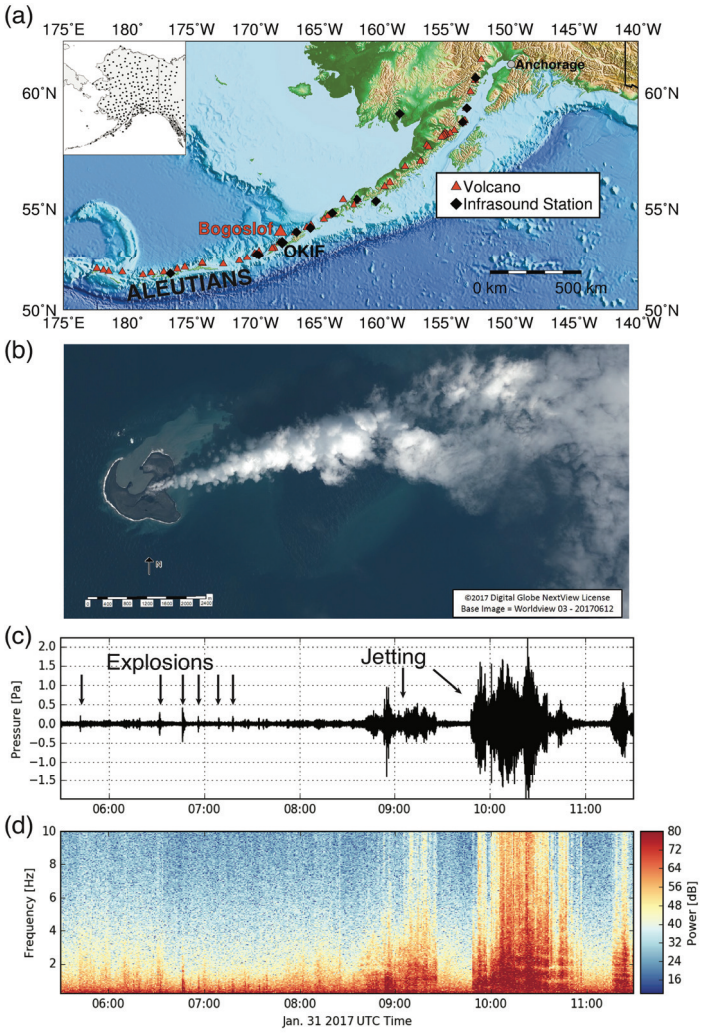

Figure 2. a: *Map of historically active Alaska volcanoes and current infrasound stations.* ***Inset****: 210 EarthScope Transportable Array (TA) colocated seismic and infrasound stations spread across Alaska.* ***b:*** *Satellite image of Bogoslof volcano, Alaska, in June 2017. Image courtesy of Alaska Volcano Observatory (AVO)/US Geological Service (USGS). Image data acquired with the Digital Globe NextView License. The 0.5- to 5-Hz filtered waveforms (**c**) and spectrogram (in dB re 20 μPa; **d**) for the January 31, 2017, eruption of Bogoslof as recorded on an infrasound array 60 km away (named OKIF).*

been established in Alaska with 210 seismo-acoustic stations at roughly 85 km spacing (**Figure 2a**, ***inset***), bringing the densest ever seismo-acoustic network to one of the world's most active volcanic regions.

Explosive Volcanic Eruptions

Volcanism occurs in a great variety of styles, ranging from so-called *effusive* processes (a passive outpouring of lava onto the Earth's surface, such as the lava flows that are exemplified by Hawaiian volcanoes) to highly *explosive* (violent, energetic eruptions such as at Mount St. Helens in 1980). Volcanoes erupt explosively because trapped volatiles (mostly water, CO_2, and SO_2) rapidly come out of solution and undergo huge volume expansions as magma ascends

from depth to the surface and depressurizes. For example, at depth in the Earth, a 1-m^3 volume of a common magma (rhyolite) at 900°C may contain about 5 percent water by weight. As this magma approaches the surface, this quantity of water would expand enormously to about 670 m^3 of vapor (Sparks et al., 1997). The degree of explosivity of a volcano is thus controlled to the first order by two main factors: volatile content and magma viscosity (low-viscosity magmas allow volatiles to escape more easily; high-viscosity magmas resist volatile escape and allow larger pressures to build).

Low-viscosity magmas characteristically exhibit long-lived effusive eruptions punctuated by short explosive bursts, along with occasional gas-rich lava fountaining episodes. On the other end of the spectrum, high-viscosity magmas and magmas containing a high concentration of volatiles typically erupt explosively. It is these eruptions, most commonly associated with the tall, steep-sided volcanoes termed *stratovolcanoes* (e.g., Mount Fuji, Mount St. Helens, Mount Vesuvius) that send up the tall eruptive columns of ash into the atmosphere that can endanger aircraft (these eruption columns are called *plinian* eruption columns). Interactions of magma with subsurface groundwater systems at volcanoes can also have explosive results.

Seismo-Acoustic Signatures of Explosive Volcanic Eruptions

Explosive eruptions are seismo-acoustic phenomena, generating large-amplitude acoustic (infrasound) and seismic waves, with the infrasound commonly recorded out to greater distances (**Figure 3**). Volcano-seismic disturbances that precede eruptions (e.g., **Figure 3a**) are thought to be produced by a variety of processes, including interactions between subsurface magma and water, magma degassing, the brittle behavior of the magma itself, and ordinary earthquake faulting processes in solid rock related to magma movement and pressure changes (Chouet and Matoza, 2013). Seismic signals are also produced by the explosive eruption itself, as magma *fragments* (breaks into small pieces) and ash columns are ejected through volcanic vents and craters. The typical seismic expression of a sustained explosive eruption is a broadband signal (~0.1 to 20 Hz) called *eruption tremor*. Seismic signals that precede and accompany eruptions usually have a limited propagation distance, typically a few tens of kilometers or up to a few hundred kilometers for larger eruptions. In contrast, similar-sized explosive eruptions produce powerful broadband (~0.01 to 20 Hz) infrasound signals (**Figure 3b**) that can be ducted efficiently

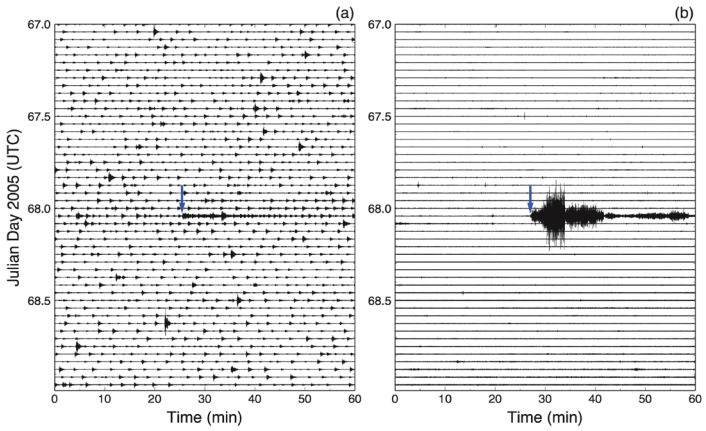

Figure 3. *Seismic vertical component velocity (**a**) and infrasonic pressure (**b**) recordings of the March 9, 2005 (Julian day 68), phreatic (steam-driven) explosion of Mount St. Helens, Washington, USA. Forty-eight hours of waveform data are shown, beginning at 00:00 on March 8, 2005 (day 67). The broadband seismometer was colocated with the central element of a 4-element infrasound array in a quiet forest site ~13.4 km from the source (Matoza et al., 2007). In each case, we show data from ±1 day spanning the event on March 9, 2005 (day 68), at ~01:26:17 UTC (**blue arrows**). The seismic tremor accompanying the phreatic explosion has a similar amplitude to seismicity before and after. A large unambiguous infrasound signal delineates the explosive eruption timing (Matoza et al., 2007). See text for further discussion.*

over long ranges (thousands of kilometers) in atmospheric waveguides. These infrasound signals are now routinely detected on sparse ground-based infrasound networks such as the IMS. In remote volcanic regions, infrasound is sometimes the only ground-based technology to record an explosive eruption and can therefore provide vital information to complement satellite data and estimate ash-release parameters for improving aviation safety. At seismically instrumented volcanoes, infrasound data reduce ambiguity in explosion detection by clearly delineating the timing and duration of the explosive eruption. This is particularly useful when the volcano is visually obscured by cloud cover.

An example of how seismic and infrasound recordings complement one another is shown in **Figure 3**, which displays seismic and infrasound waveforms from a colocated seismo-acoustic station deployed 13.4 km from Mount St. Helens volcano, Washington, USA (Matoza et al., 2007). This is called a *helicorder* plot and mimics traditional seismograph recordings that were originally made on a piece of paper wrapped around a rotating drum. Time progresses from the upper left in the figure to the lower right, with each 60-minute waveform progressing from left to right in the figure and the next 60-minutes plotted directly below. Mount St. Helens underwent continuous eruptive activity from 2004 to 2008.

The figure shows a 2-day record around a *phreatic* (steam-driven) explosion that occurred on March 9, 2005 (all times

reported in Universal Time [UT]). The seismometer (**Figure 3a**) records a near-continuous sequence of rhythmic volcano-seismic disturbances called long-period events (LPs), a volcano-seismology term that refers to signals with dominant frequencies from 0.5 to 5 Hz. At the beginning of the plot before the steam explosion, the LPs occur in cyclic regularity, with a prominent peak in the interevent time distribution (Matoza and Chouet, 2010). During the steam explosion that begins on March 9, 2005 (day 68), at 01:26:17 (**Figure 3a, *blue arrow***), the seismic LPs merge closer together in time and transition into continuous eruption tremor as fluid (primarily steam and entrained ash) is ejected into the atmosphere. After the steam explosion, the LP rate decelerates and returns to the background rate within about 90 minutes.

The 2004-2008 eruption of Mount St. Helens was closely monitored with multiple types of instrumentation. Thus, we have accurate knowledge of how the seismic recordings relate to the eruption process. However, without any other data, it might have been difficult to determine exactly when (and even if) an explosive eruption had occurred because similar seismic sequences as those shown in **Figure 3a** can be recorded even in the absence of an explosive eruption. However, the infrasound data (**Figure 3b**) reduce this ambiguity and provide clear evidence that an eruption has occurred (Matoza et al., 2007). Before and after the steam explosion, the infrasound data record only ambient noise. A clear signal begins coincident with the ejection of fluid into the atmosphere and continues to indicate the sustained jetting of fluid for a total of about 53 minutes. Thus, the infrasound data delineate the timing and duration of the explosive eruption process.

Long-Range Atmospheric Propagation of Volcanic Infrasound

Low-frequency sound from volcanoes has long been known to propagate great distances. The powerful 1883 Krakatoa (located in present-day Indonesia) eruption produced acoustic-gravity waves that circumnavigated the globe multiple times and were recorded on weather barometers (Gabrielson, 2010). Long-range infrasound propagation occurs for two main reasons. First, absorption is relatively low at these frequencies, about 5×10^{-5} dB/km at 1 Hz compared with about 2 dB/km at 500 Hz (Sutherland and Bass, 2004). Second, strong vertical gradients in the temperature and horizontal winds create infrasonic waveguides in the troposphere (approximately 0 to 15 km altitude), stratosphere (approximately 15 to 60 km), and thermosphere (approximately 85 to 120 km). Substantial spatiotemporal atmospheric variability, particularly changes in wind speed and direction, create variability and complexity in infrasound propagation. For example, numerous studies have found that the seasonal stratospheric winds (typically blowing to the east in the winter hemisphere and to the west in the summer hemisphere) largely control global infrasound propagation and detection (e.g., Le Pichon et al., 2009). Moreover, there has recently been a focus on creating better, more accurate, and seamless atmospheric models from the ground through the thermosphere to more accurately model infrasound propagation at long ranges (Blanc et al., 2017). Similarly, because long-range infrasound propagation is sensitive to wind and temperature changes, certain volcanoes that radiate infrasound near continuously have shown promise as a tool to passively detect changes in atmospheric structure that would otherwise be unobservable (e.g., Assink et al., 2013).

Remote Detection of Volcanic Infrasound

The data shown in **Figure 3** were collected as part of a project to evaluate the potential of remote infrasound arrays to provide useful information about explosive eruptions (Garces et al., 2008). In addition to the local data shown from Mount St. Helens, an identical infrasound array was deployed approximately 250 km to the east, at a location where infrasound ducted in the stratosphere can be expected to return to the ground during typical winter conditions (Matoza et al., 2007). Similar waveforms were recorded at the near and distant arrays, indicating that remote infrasound observations can represent an accurate record of the source. The utility of long-range infrasound signals has been confirmed by numerous observations of eruption signals on remote infrasound arrays.

Larger and more energetic eruptions produce more powerful infrasound signals that can be recorded farther from the source. The June 2009 eruption of Sarychev Peak volcano on a remote, uninhabited island in the Kurile Islands (a volcanic island chain stretching between Japan and the Kamchatka Peninsula of Russia) provides an illustrative example (Matoza et al., 2011; **Figure 4**). Due to the remote location, local ground-based geophysical observations were nonexistent and the eruption did not register on any remote seismic stations (e.g., seismic stations at distances of 352 km, 512 km, and 800 km). The first indication that an eruption had occurred was in satellite data acquired on June 11, 2009, that showed a thermal anomaly and weak ash emissions. Subsequently, at 22:16 on June 12, 2009, spectacular photographs

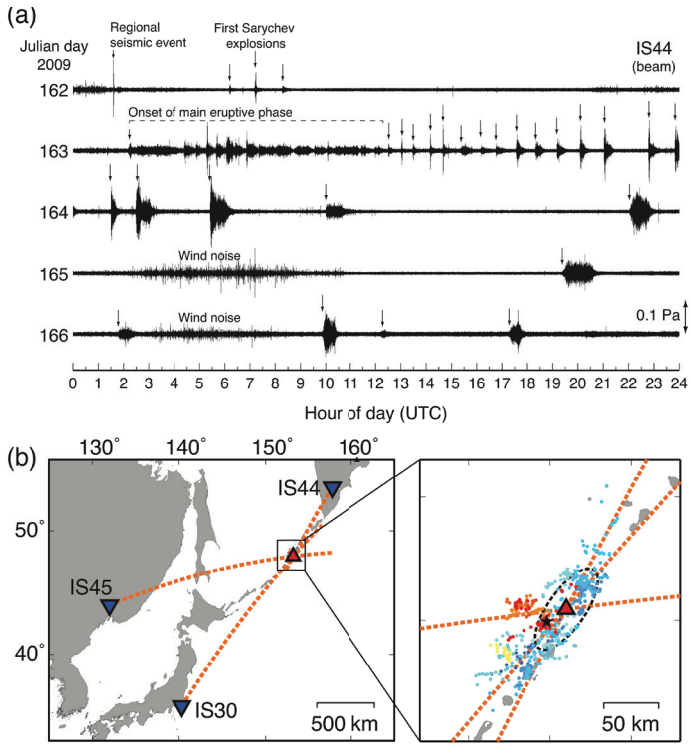

Figure 4. a: *Infrasonic waveforms recorded at IMS station IS44 (Kamchatka) for the June 2009 eruption of Sarychev Peak, Kurile Islands (5 days: June 11-16, 2009, or Julian days 162-167 2009). Each waveform shows one full day of data. Infrasound array data have been beamformed (waveforms aligned and stacked for azimuth of Sarychev Peak and acoustic velocity) using a time-delay beamformer and filtered 0.5-5 Hz.* ***Arrows*** *mark the beginning of signals from individual explosive eruptions from the volcano.* ***b:*** *Infrasonic source location for the June 2009 eruption of Sarychev Peak (**large red triangle**) via back-azimuth cross bearings using the closest three IMS arrays: IS44, IS45, and IS30 (**inverted blue triangles**). The source location solutions (**dots**) are colored as a function of time.* ***Black star,*** *mean source centroid.* ***Dashed ellipse*** *shows 90% confidence for source location. Modified from Matoza et al. (2011), with permission.*

of an eruption column issuing from the volcano were taken by astronauts aboard the International Space Station who just happened to be passing by (**Figure 5**). These unique photographs also captured ash dispersed at altitude from previous eruptions and pyroclastic flows in the process of descending the mountain (*pyroclastic flows* are rapid ground-hugging flows of hot gas and volcanic debris; the term *pyroclastic* is derived from the Greek words for "fire" and "broken" and refers to material that is erupted explosively from a volcano). Whereas remote seismic stations did not record the Sarychev Peak eruption, infrasound signals registered at 7 infrasound arrays located at distances from ~640 to 6,400 km (Matoza et al., 2011). **Figure 4a** shows infrasound waveforms at IMS station IS44, located 643 km from Sarychev Peak in Petropavlovsk-Kamchatsky, Kamchatka, Russia. Retrospective analysis shows that the remote IS44 infrasound waveforms provide a detailed record of the explosion chronology that

Figure 5. *NASA photograph of the June 2009 eruption of Sarychev Peak, Kurile Islands, taken by astronauts aboard the International Space Station. The image shows the vertical plinian eruption column and simultaneous ground-hugging pyroclastic flows descending the mountain. The smooth white cloud at the top of the eruption column has been interpreted as a pileus cloud, that is, water condensation resulting from rapid rising and cooling of the air mass above the eruption column. Image from NASA's Earth Observatory. For more information and an animation of image sequences, see* https://earthobservatory.nasa.gov/IOTD/view.php?id=38985.

has higher temporal resolution than was possible to derive with the available satellite data (much of the eruption was obscured in satellite data by a meteorological cloud layer). In addition, by combining the direction-of-arrival (back-azimuth) information at multiple arrays, it is possible to locate the source using back-azimuth cross bearings. By modeling atmospheric propagation paths using 3-D ray tracing with atmospheric specifications from the European Centre for Medium-Range Weather Forecasting (ECMWF), it is possible to locate the source using the 3 closest arrays to within 15 km of the true source location. The source-location error ellipse of ~100 km likely results from unresolved details of atmospheric propagation, source complexity, and back-azimuth estimation uncertainty (**Figure 4b**).

Source Mechanisms of Volcanic Infrasound

We have shown examples of how infrasound recordings at local (<15 km), regional (15-250 km), and global (>250 km) distances from volcanoes can be used to detect, locate, and provide detailed chronologies of explosive eruptions. These acoustic constraints on the basic parameters of explosive eruptions are already improving the prediction accuracy of numerical models of ash transport and dispersal and aiding with aviation safety. Ongoing research aims to better understand the source mechanism of volcanic infrasound, with the goal of providing detailed, quantitative parameters of the eruption based on infrasound observations.

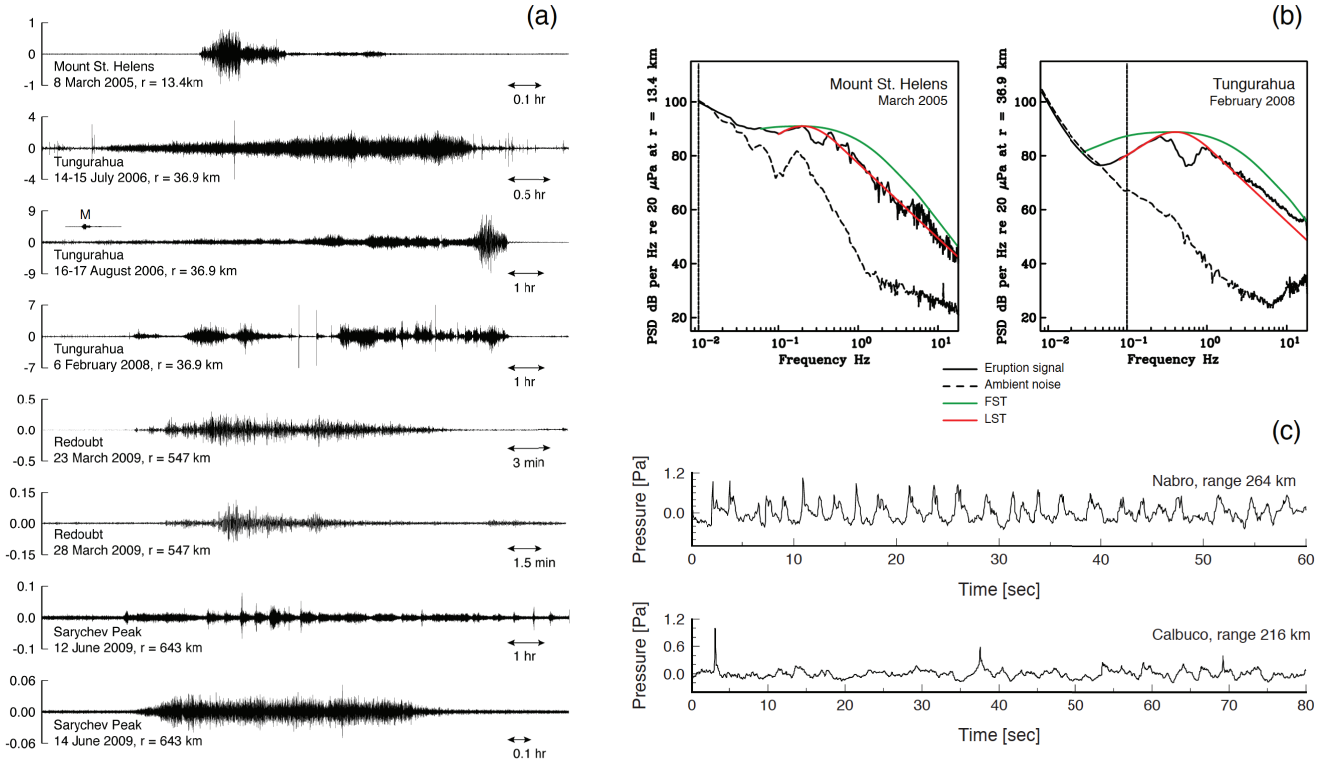

Figure 6. a: *Example infrasound waveforms from sustained explosive volcanic eruptions. Scale bars (**right**) indicate time scale for each waveform (e.g., for the top waveform from Mount St. Helens, the time between the arrowheads is 0.1 hour). y-Axis, acoustic pressure (in Pa). Each trace is annotated with the name of the volcano, date of eruption, and infrasound recording range (r). "M" on third axis is the Mount St. Helens signal (**top trace**) at the same scale for comparison.* ***b:*** *Comparison of infrasound pressure power spectral density (PSD) to the jet-noise similarity spectra (Tam et al., 1996; Matoza et al., 2009). FST, fine-scale turbulence spectrum; LST, large-scale turbulence spectrum (the two types of jet mixing noise).* ***Solid lines,*** *eruption signals;* ***dashed lines,*** *samples of the ambient noise before the eruption signal.* ***c:*** *Example long-range infrasound from eruptions at Nabro volcano, Eritrea, and Calbuco volcano, Chile, showing asymmetric positively skewed waveforms similar to those associated with the crackle phenomenon in audible jet noise from jet engines and rockets.*

Significant progress in understanding volcano infrasound has been made through dedicated local deployments in tandem with other observation systems (e.g., seismometers, visual and thermal cameras, gas sensors, ground deformation sensors). Recordings of volcanic infrasound have now been made at numerous volcanoes worldwide (Fee and Matoza, 2013). As described in **Explosive Volcanic Eruptions**, volcanism is highly variable, representing a spectrum of processes ranging from effusive to explosive behavior. Consequently, volcanoes produce a great diversity of infrasound source mechanisms and signals.

Infrasound is thought to be produced by resonance in shallow magma and gas-filled cavities; by explosive bursts of large bubbles of gas (called "slugs") at the magma surface in low-viscosity magmas; by explosive magma-water interactions; by the sudden explosive failure of a solid cap rock that was sealing a pressurized gas pocket; by sustained turbulent flow of ash-laden gas jets in the atmosphere; by turbulent ground-hugging pyroclastic flows of dense hot gas and particles; and by rock falls, mudflows, and explosive blowout of gas-charged blocks, just to name some examples. The duration of volcano-infrasound waveforms ranges from short-duration events lasting ~1 second to sustained tremor signals lasting months to years (tremor is a catchall term for sustained signals, as differentiated from transient signals). Amplitudes span a wide dynamic range, from small signals approaching the noise level of infrasound sensors (on the order of millipascals) to larger explosions producing nonlinear shock waves with overpressures exceeding atmospheric pressure ($>10^5$ Pa). Topography and volcanic crater morphology modify the signals and create additional variety in the observed waveforms. Despite source process diversity and waveform complexity, wavefield modeling and inversion techniques have been used to infer eruption source parameters and processes (Fee and Matoza, 2013).

Effusive eruptions and roiling lava lakes have been observed to produce near-continuous broadband and/or harmonic infrasound with pronounced spectral peaks. Kilauea Volcano, Hawai'i, is a well-studied example, with prodigious broadband and harmonic infrasonic tremor and occasional short-duration explosions. Cavities and gas-filled conduits above degassing magma bodies also appear to substantially shape

the infrasonic signature. In one example, a ~200-m deep gas-filled cavity above the Halema'uma'u lava lake at Kilauea, Hawai'i, was successfully modeled as a large Helmholtz resonator producing a sustained spectral peak at ~0.5 Hz (Fee et al., 2010). Flow-induced oscillations through shallow volcanic cavity structures have also been hypothesized as a source of harmonic infrasound (Matoza et al., 2010). Although of interest for improving understanding of how Hawaiian volcanoes work and contributing to local volcano monitoring systems, these types of signals are generally weaker and do not tend to propagate long distances in the atmosphere.

At the other end of the spectrum is explosive volcanism. However, even within the general category of "explosive volcanism," there is a great variety of processes and infrasound signals. These processes range from discrete blasts lasting only a few seconds to sustained jetting activity that can last for tens of minutes to hours in duration (**Figure 6a**).

Perhaps the most well-known explosive eruption style is termed *plinian*, which produces the tall eruptive columns of pyroclasts reaching high in the atmosphere, first described by Pliny the Younger for the AD 79 eruption of Vesuvius. Volcanologists schematically divide plinian eruption columns into three altitude regions. The lowermost section of a plinian volcanic eruption column represents a momentum-driven, turbulent, free-shear jet flow. Above the jet-flow region (termed the *gas-thrust* region), the flow transitions with altitude into a thermal buoyancy-driven volcanic *plume* (the *convective* region), which rises higher in the atmosphere by entraining surrounding air (**Figure 5**). Eventually, neutral buoyancy is achieved and the flow transitions into a laterally spreading *umbrella region* dominated by advection and diffusion.

Recent work has suggested that the gas-thrust region of plinian eruptions, a large natural jet flow, generates a low-frequency (infrasonic) form of the aeroacoustic jet noise produced by smaller scale anthropogenic jets, such as the exhausts of jet engines and rockets (Matoza et al., 2009, 2013; Fee et al., 2013; Taddeucci et al., 2014). Jet noise is the noise generated by a turbulent jet flow itself. Jet noise has been characterized in laboratory and field aeroacoustics studies by considering how acoustic signal properties vary as a function of angle to the jet axis and jet operating parameters such as the jet velocity, diameter, temperature, density, and nozzle geometry. The spectral shapes of observed volcano infrasound signals are in approximate agreement with the spectra of laboratory jets but shifted to lower frequencies (Matoza et al., 2009; **Figure 6b**). However, the observed volcanic signals have additional complexities not present in the pure-air laboratory data. These features may result from multiphase flow containing solid particles and liquid droplets, very high temperatures, and complex volcanic vent morphology (Matoza et al., 2013). In addition, similarity between waveforms from volcanic eruption infrasound and jet flow from supersonic jet engines and solid rocket motors has been observed (Fee et al., 2013). Eruptions from Nabro volcano, Eritrea; Stromboli volcano, Italy; and Calbuco volcano, Chile, produced infrasound waveforms consisting of asymmetric, shock-like pressure pulses with positive waveform skewness, similar to those associated with the "crackle" phenomenon in audible noise from supersonic, heated jet and rocket engines (Gee et al., 2007; Fee et al., 2013; Goto et al., 2014; **Figure 6c**). High-speed visual (Yokoo and Ishihara, 2007; Genco et al., 2014) and infrared (Delle Donne and Ripepe, 2012) video has been employed to image supersonic shock waves emanating from explosions and reconstruct the resultant acoustic waves. Differencing of images from sustained volcanic jets has revealed repeated shock waves emanating from the edges of the jet (Genco et al., 2014; Taddeucci et al., 2014).

The infrasound produced by volcanic jet flows is in some ways similar, but is not perfectly analogous, to the jet noise produced by laboratory jets and flight-vehicle exhaust. To further develop understanding of volcanic jet aeroacoustics, laboratory (e.g., Médici and Waite, 2016) and numerical (e.g., Cerminara et al., 2016) studies are required. Laboratory and numerical studies will also need to be coupled with novel field deployments that improve observational constraints on volcanic jet noise. For instance, volcanic jet flows are vertically oriented, such that sampling directivity in the acoustic wavefield of a volcanic jet is challenging. Infrasound sensors are usually located on the ground surface and thus sample the acoustic wavefield in a limited angular range in the upstream jet direction.

Toward this goal, a recent field experiment employed infrasound sensors aboard a tethered aerostat (a helium balloon-kite hybrid) at the active Yasur volcano, Vanuatu (Jolly et al., 2017). The aerostats carried 2-3 infrasound sensors suspended on a string with 10-20 m vertical spacing, with each aerostat deployment lasting ~20 min to an hour. The sensors were lofted to a position ~200 to 300 m above the active vent and <100 m above the crater rim at 38 tethered positions, sampling angular ranges of ~200° in azimuth and ~50° in takeoff angle. Comparison with synchronous recordings of ground-based infrasound sensors enabled determination of an anisotropic radiation pattern that may be related to path effects from the crater walls and/or source directional-

ity. Yasur volcano was chosen for this experiment because it is highly active and offered the chance to test the novel aerostat-based acquisition system. The coincident ground-based seismo-acoustic deployment lasted only about 8 days but recorded more than 8,000 infrasound explosion signals and more than 10,000 volcanic earthquakes. Infrasound signals exceeded 500 Pa at 300 m from the vent.

Current State of Volcano Infrasound Monitoring

At present, numerous volcano observatories are using infrasound to detect, locate, and characterize volcanic eruptions. The recent eruption of Bogoslof volcano, Alaska (**Figure 2**), produced over 60 powerful explosions in a span of 8 months (see www.avo.alaska.edu). No local monitoring was possible due to the hazard and small size of this remote island, yet each eruption produced volcanic emissions that posed a danger to aircraft, passing ships, and a nearby fishing port. In conjunction with seismic, satellite, and lightning data, AVO used data from multiple infrasound arrays in the region, at distances from 60 to 820 km, to detect and characterize eruptions in near-real-time. Automated array-processing algorithms enabled detection of both short-duration explosions and longer duration jetting, with relevant AVO personnel receiving eruption alerts via text message and email. Infrasound was particularly useful in this scenario due to the remoteness of Boglosof and the complex nature of this eruption.

Figure 2, c and **d**, shows the waveforms and spectrogram of a Bogoslof eruption on January 31, 2017, as detected on an infrasound array (named OKIF) on Umnak Island 60 km away. The eruption begins with a number of short-duration, impulsive explosions and then transitions to multiple jetting phases. AVO observed these various eruptive phases in near-real-time and inferred a change in eruption style from subaqueous to subaerial that was later found to be consistent with other observations. The source depth is a key component used in estimating the volcanic emissions hazard.

Major progress has been made in using infrasound to understand and monitor volcanic eruptions, and the technology has matured into an essential tool for many volcano scientists. However, numerous questions remain. Quantitative source models are only available for a limited range of volcanic processes. Further developed quantitative models of the infrasonic source have the potential to improve estimates of critical eruption characteristics such as the amount, location, and type of volcanic emissions. Infrasound propagation modeling also continues to improve through refinements in atmospheric specifications and numerical models and through increases in computational capacity. For example, wind is often neglected in full-waveform infrasonic modeling but can significantly affect the wave propagation. Dense networks of high-quality infrasound sensors deployed at various distances and azimuths from the volcanic vent will provide valuable data to test source and propagation models. Continued development of algorithms for local and remote automated detection, association, and location of volcanic eruption infrasound signals will improve hazard monitoring.

Acknowledgments

This work was supported by National Science Foundation Grants EAR-1614855, EAR-1620576, EAR–1614323, and EAR-1331084. We thank Editor Arthur Popper for helpful comments.

References

Assink, J. D., Waxler, R., Frazier, W. G., and Lonzaga, J. (2013). The estimation of upper atmospheric wind model updates from infrasound data. *Journal of Geophysical Research* 118, 1-18. https://doi.org/10.1002/jgrd.50833.

Blanc, E., Ceranna, L., Hauchecorne, A., Charlton-Perez, A., Marchetti, E., Evers, L. G., Kvaerna, T., Lastovicka, J., Eliasson, L., Crosby, N. B., Blanc-Benon, P., Le Pichon, A., Brachet, N., Pilger, C., Keckhut, P., Assink, J. D., Smets, P. S. M., Lee, C. F., Kero, J., Sindelarova, T., Kämpfer, N., Rüfenacht, R., Farges, T., Millet, C., Näsholm, S. P., Gibbons, S. J., Espy, P. J., Hibbins, R. E., Heinrich, P., Ripepe, M., Khaykin, S., Mze, N., and Chum, J. (2017). Toward an improved representation of middle atmospheric dynamics thanks to the ARISE Project. *Surveys in Geophysics* 1-55. https://doi.org/10.1007/s10712-017-9444-0.

Casadevall, T. J. (1994). *Volcanic Ash and Aviation Safety: Proceedings of the First International Symposium on Volcanic Ash and Aviation Safety*, Seattle, WA, July 1991. US Geological Survey Bulletin 2047, US Government Printing Office, Washington, DC.

Cerminara, M., Ongaro, T. E., and Neri, A. (2016). Large eddy simulation of gas-particle kinematic decoupling and turbulent entrainment in volcanic plumes. *Journal of Volcanology and Geothermal Research* 326, 143-171. https://doi.org/10.1016/j.jvolgeores.2016.06.018.

Chouet, B. A., and Matoza, R. S. (2013). A multi-decadal view of seismic methods for detecting precursors of magma movement and eruption. *Journal of Volcanology and Geothermal Research* 252, 108-175. https://doi.org/10.1016/j.jvolgeores.2012.11.013.

Christie, D., and Campus, P. (2010). The IMS infrasound network: Design and establishment of infrasound stations. In Le Pichon A., Blanc, E., and Hauchecorne, A. (Eds.), *Infrasound Monitoring for Atmospheric Studies.* Springer, The Netherlands, chap. 2, pp. 29-75.

Delle Donne, D., and Ripepe, M. (2012). High-frame rate thermal imagery of Strombolian explosions: Implications for explosive and infrasonic source dynamics. *Journal of Geophysical Research: Solid Earth* 117 B9. https://doi.org/10.1029/2011JB008987.

Fee, D., Garces, M., Patrick, M., Chouet, B., Dawson, P., and Swanson, D. (2010). Infrasonic harmonic tremor and degassing bursts from Halema'uma'u Crater, Kilauea Volcano, Hawaii. *Journal of Geophysical Research: Solid Earth* 115 B11316. https://doi.org/10.1029/2010JB007642.

Fee, D., and Matoza, R. S. (2013). An overview of volcano infrasound: From Hawaiian to Plinian, local to global. *Journal of Volcanology and Geothermal Research* 249, 123-139. https://doi.org/10.1016/j.jvolgeores.2012.09.002.

Fee, D., Matoza, R. S., Gee, K. L., Neilsen, T. B., and Ogden, D. E. (2013). Infrasonic crackle and supersonic jet noise from the eruption of Nabro Volcano, Eritrea. *Geophysical Research Letters* 40, 1-5. https://doi.org/10.1002/grl.50827.

Gabrielson, T. B. (2010). Krakatoa and the Royal Society: The Krakatoa explosion of 1883. *Acoustics Today* 6(2), 14-19.

Garces, M., Fee, D., McCormack, D., Servranckx, R., Bass, H., Hetzer, C., Hedlin, H., Matoza, R., Yepes, H., and Ramon, P. (2008). Capturing the acoustic fingerprint of stratospheric ash injection. *EOS Transactions American Geophysical Union* 89(40), 377-379. https://doi.org/10.1029/2008EO400001.

Gee, K. L., Sparrow, V. W., Atchley, A., and Gabrielson, T. B. (2007). On the perception of crackle in high-amplitude jet noise. *AIAA Journal* 45(3), 593-598. https://doi.org/10.2514/1.26484.

Genco, R., Ripepe, M., Marchetti, E., Bonadonna, C., and Biass, S. (2014). Acoustic wavefield and Mach wave radiation of flashing arcs in strombolian explosion measured by image luminance. *Geophysical Research Letters* 41(20), 7135-7142. https://doi.org/10.1002/2014GL061597

Global Volcanism Program. (2013). *Volcanoes of the World*, v. 4.5.3, edited by Venzke, E., Department of Mineral Sciences, National Museum of Natural History, Smithsonian Institution, Washington, DC. Available at http://dx.doi.org/10.5479/si.GVP.VOTW4-2013. Accessed June 2016.

Goto, A., Ripepe, M., and Lacanna, G. (2014). Wideband acoustic records of explosive volcanic eruptions at Stromboli: New insights on the explosive process and the acoustic source. *Geophysical Research Letters* 41, 3851–3857. https://doi:10.1002/2014GL060143.

Jolly, A. D., Matoza, R. S., Fee, D., Kennedy, B. M., Iezzi, A. M., Fitzgerald, R. H., Austin, A. C., and Johnson, R. (2017). Capturing the acoustic radiation pattern of strombolian eruptions using infrasound sensors aboard a tethered aerostat, Yasur volcano, Vanuatu. *Geophysical Research Letters* 44(19), 9672-9680. https://doi.org/10.1002/2017GL074971.

Le Pichon, A., Vergoz, J., Blanc, E., Guilbert, J., Ceranna, L., Evers, L., and Brachet, N. (2009). Assessing the performance of the International Monitoring System's infrasound network: Geographical coverage and temporal variabilities. *Journal of Geophysical Research: Atmospheres* 114, D08112. https://doi.org/10.1029/2008JD010907.

Matoza, R. S., and Chouet, B. A. (2010). Subevents of long-period seismicity: Implications for hydrothermal dynamics during the 2004-2008 eruption of Mount St. Helens. *Journal of Geophysical Research: Solid Earth* 115, B12206. https://doi.org/10.1029/2010JB007839.

Matoza, R. S., Fee, D., and Garces, M. A. (2010). Infrasonic tremor wavefield of the Pu'u O'o crater complex and lava tube system, Hawaii, in April 2007. *Journal of Geophysical Research: Solid Earth* 115, B12312. https://doi.org/10.1029/2009JB007192.

Matoza, R. S., Fee, D., Garces, M. A., Seiner, J. M., Ramon, P. A., and Hedlin, M. A. H. (2009). Infrasonic jet noise from volcanic eruptions. *Geophysical Research Letters* 36, L08303, https://doi.org/10.1029/2008GL036486.

Matoza, R. S., Fee, D., Neilsen, T. B., Gee, K. L., and Ogden, D. E. (2013). Aeroacoustics of volcanic jets: Acoustic power estimation and jet velocity dependence. *Journal of Geophysical Research: Solid Earth* 118, 6269-6284. https://doi.org/10.1002/2013JB010303.

Matoza, R. S., Green, D. N., Le Pichon, A., Shearer, P. M., Fee, D., Mialle, P., and Ceranna, L. (2017). Automated detection and cataloging of global explosive volcanism using the International Monitoring System infrasound network, *Journal of Geophysical Research: Solid Earth* 122, 2946–2971. https://doi.org/doi:10.1002/2016JB013356.

Matoza, R. S., Hedlin, M. A. H., and Garces, M. A. (2007). An infrasound array study of Mount St. Helens. *Journal of Volcanology and Geothermal Research* 160, 249-262. https://doi.org/10.1016/j.jvolgeores.2006.10.006.

Matoza, R. S., Le Pichon, A., Vergoz, J., Herry, P., Lalande, J., Lee, H., Che, I., and Rybin, A. (2011). Infrasonic observations of the June 2009 Sarychev Peak eruption, Kuril Islands: Implications for infrasonic monitoring of remote explosive volcanism. *Journal of Volcanology and Geothermal Research*, 200, 35-48. https://doi.org/10.1016/j.jvolgeores.2010.11.022.

Médici, E. F., and Waite, G. P. (2016). Experimental laboratory study on the formation of multiple shock waves observed during volcanic eruptions. *Geophysical Research Letters* 43(1), 85-92. https://doi.org/10.1002/2013GL058340

National Academies of Sciences, Engineering, and Medicine. (2017). *Volcanic Eruptions and Their Repose, Unrest, Precursors, and Timing*. The National Academies Press, Washington, DC. https://doi.org/10.17226/24650.

Sparks, R. S. J., Bursik, M. I., Carey, S. N., Gilbert, J., Glaze, L. S., Sigurdsson, H., and Woods, A. W. (1997). *Volcanic Plumes*. Wiley, Chichester, UK.

Sutherland, L. C., and Bass, H. E. (2004). Atmospheric absorption in the atmosphere up to 160 km. *The Journal of the Acoustical Society of America* 115(3), 1012-1032. https://doi.org/10.1121/1.1631937.

Taddeucci, J., Sesterhenn, J., Scarlato, P., Stampka, K., Del Bello, E., Pena Fernandez, J. J., and Gaudin, D. (2014). High-speed imaging, acoustic features, and aeroacoustic computations of jet noise from Strombolian (and Vulcanian) explosions. *Geophysical Research Letters* 41(9), 2014GL059925. https://doi.org/10.1002/2014GL059925.

Tam, C. K. W., Golebiowski, M., and Seiner, J. M. (1996). On the two components of turbulent mixing noise from supersonic jets. *American Institute of Aeronautics and Astronautics Paper* 96-1716.

Yokoo, A., and Ishihara, K. (2007). Analysis of pressure waves observed in Sakurajima eruption movies. *Earth Planet Space* 59(3), 177-181.

Biosketches

Robin Matoza is an assistant professor of geophysics at the Department of Earth Science, University of California, Santa Barbara. He received an MGeophys from the University of Leeds, UK, in 2004 and a PhD in Earth sciences at the Institute of Geophysics and Planetary Physics (IGPP), Scripps Institution of Oceanography, La Jolla, CA, in 2009. He was a postdoctoral researcher at the Commissariat à l'énergie atomique (CEA), France, and a Cecil H. and Ida M. Green Scholar at IGPP. His research is focused on understanding the seismic and infrasonic signatures of volcanic unrest and eruption, with application in monitoring and mitigating volcanic hazards.

David Fee is a research associate professor at the Geophysical Institute, University of Alaska Fairbanks. He also works at the Alaska Volcano Observatory and the Wilson Alaska Technical Center. Dr. Fee obtained his MS in seismology from the University of Wyoming, Laramie in 2004, and PhD in volcano infrasound from the University of Hawai'i at Manoa in 2010. Dr. Fee's research focuses on using infrasound and seismology to study volcanic eruptions and anthropogenic explosions. He also assists with the operation and maintenance of numerous stations of the Comprehensive Nuclear-Test-Ban Treaty Organization's International Monitoring System.